



HAL
open science

Battery Storage System Optimal Exploitation Through Physics-Based Model Predictive Control

Emil Namor, Fabrizio Sossan, Dimitri Torregrossa, Rachid Cherkaoui, Mario Paolone

► **To cite this version:**

Emil Namor, Fabrizio Sossan, Dimitri Torregrossa, Rachid Cherkaoui, Mario Paolone. Battery Storage System Optimal Exploitation Through Physics-Based Model Predictive Control. 2017 IEEE Manchester PowerTech, Jun 2017, Manchester, United Kingdom. pp.1-6. hal-02108823

HAL Id: hal-02108823

<https://hal.science/hal-02108823>

Submitted on 24 Apr 2019

HAL is a multi-disciplinary open access archive for the deposit and dissemination of scientific research documents, whether they are published or not. The documents may come from teaching and research institutions in France or abroad, or from public or private research centers.

L'archive ouverte pluridisciplinaire **HAL**, est destinée au dépôt et à la diffusion de documents scientifiques de niveau recherche, publiés ou non, émanant des établissements d'enseignement et de recherche français ou étrangers, des laboratoires publics ou privés.

Battery Storage System Optimal Exploitation Through Physics-Based Model Predictive Control

Emil Namor, Fabrizio Sossan, Dimitri Torregrossa, Rachid Cherkaoui, Mario Paolone
Distributed Electrical Systems Laboratory

École Polytechnique Fédérale de Lausanne, Switzerland

{emil.namor, fabrizio.sossan, dimitri.torregrossa, rachid.cherkaoui, mario.paolone}@epfl.ch

Abstract—Traditionally, the safe operation of a battery energy storage system (BESS) is achieved by imposing conservative constraints on its DC bus current and voltage. By using a computationally efficient single particle model (SPM), we propose to replace these constraints with the battery internal ion concentrations and electrical potentials in order to avoid these quantities to exceed hazardous limits. Indeed, the in-depth knowledge of the BESS internal states provided by the SPM, enhances the awareness of a control action and allows for a better exploitation of the BESS energy and power capabilities, while maintaining safe operational conditions. The target application is composed by a model predictive control (MPC) applied to a MW-class grid-connected BESS responsible to dispatch the operation of a medium voltage (20 kV) feeder interfacing heterogeneous loads and distributed generation. The performance of the proposed MPC are assessed and compared with respect to a traditional approach constraining the BESS DC bus current and voltage.

I. INTRODUCTION

The decreasing cost of Lithium-based electrochemical storage is fostering the deployment of grid-connected battery energy storage systems, which are expected to play a key role in the process of displacing electrical energy production from conventional to renewable sources. A key challenge related to the reliable operation of BESS is the development of control strategies capable to account for both their physical operational constraints and aging factors with the main objectives of reducing fault occurrences, thermal runways and the magnitude of degradation phenomena in the cells. The originating cause of Li-ion battery ageing and cell degradation is the occurrence of electrochemical parasitic reactions, such as the formation of solid electrolyte interphase (SEI) and Lithium plating. The magnitude of these phenomena depends on the evolution of the cells internal states and, in particular, overpotentials and ion concentrations in the various parts of the cell. Therefore, the knowledge of these quantities allows to implement efficient battery control policies that avoid electrochemical degradation while exploiting the full battery potential [1]–[5]. However, these quantities are not directly measurable. As a consequence, operational constraints are normally defined on those variables which are directly measurable, namely the battery terminal voltage and the current [6]–[8]. Voltage and current of individual cells are related to the internal states of the cell in a rather complex way. In order to operate the BESS in a safe domain by imposing operational limits on these

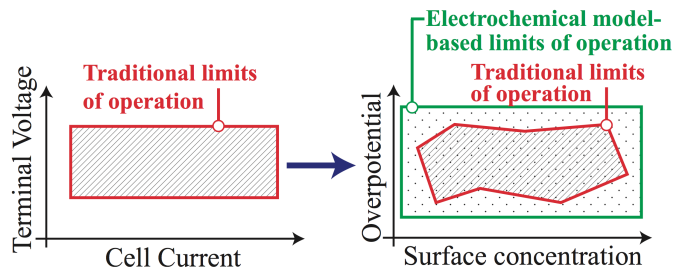


Figure 1. Qualitative comparison of the traditional operational constraints for a Li-ion cell, based on measurable quantities (left) and allowed by the knowledge of actual cell physical states (right) [4].

externally-available quantities, one should choose conservative constraints, thus preventing to operate the BESS in conditions which are not harmful. In other words, these limits reduce the power and energy capability of a BESS (see Fig. 1). A further advantage of dealing with electrochemical constraints is when considering the progressive battery aging. In fact, as the battery ages, its behavior evolves so the current/voltage constraints set for the new battery may not ensure safe operation for an aged one.

Within the above-mentioned context, we propose a model predictive control where reliable battery operation is enforced thanks to implementing electrochemical predictive constraints by relying on a physics-based (PB) model of a Li-ion cell. In this paper we make use of the single particle model (SPM) [9], [10], which, in spite of its simplicity, retains the ability to describe cells internal states and the main mechanisms of Li-ion battery aging [11].

In this paper, we assess the performances of such physics-based MPC applied to the energy management of a grid-connected BESS and compare it to a traditional approach, based on constraints on the BESS DC bus current and voltage. We show the prediction performance of the SPM and its capability to provide extensive information about the BESS state, that can be exploited by the BESS control. Finally, we show that, with respect to the classical MPC formulations [6], [7], the proposed one achieves augmented awareness and less conservative control actions, and it opens to the perspective of implementing detailed anti-ageing control policies. We quantify the advantages of such approach in terms of range

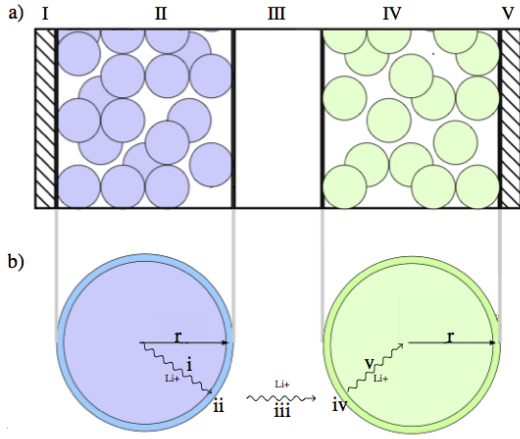


Figure 2. a) Structure of a Li-ion cell: I) negative current collector; II) anode; III) separator; IV) cathode; V) positive current collector. b) Single particle model schematic.

extension and we discuss few possible approaches to extend such framework in order to accomodate explicit anti-ageing control policies.

The paper is organized as follows: section II introduces the SPM, section III briefly describes the MPC framework and the model reformulation performed to cast the SPM in such a framework. Section IV describes the simulation setup and analyses the main results of the work. Finally, section V summarises the main results and contribution of this paper.

II. THE SINGLE PARTICLE MODEL

The model we use is extensively described in [9]. The SPM describes the intercalation dynamics of a Lithium ion cell (i.e. the diffusion within the electrode active materials) and its charge transfer phenomena. The SPM is generally accurate as long as the current rates are below 2C. Such a condition is satisfied by the majority of BESS applications in power systems.

The two electrodes of a Li-ion cell are modeled by two spherical particles. The model structure and the relevant phenomena occurring within the cell and modeled by a SPM are represented in Fig. 2. The modeled physical phenomena (and in parentheses the respective contribution to external voltage) are: i) the mass transfer (i.e. the diffusion of Lithium ions) within anode active material (anode equilibrium potential); ii) the charge transfer at the electrode electrolyte interface (anode charge transfer polarization); iii) ionic conduction in the electrolyte (ohmic voltage drop); iv) charge transfer at the electrode electrolyte interface (cathode charge transfer polarization); v) mass transfer within cathode active material (cathode equilibrium potential). This model can incorporate detailed and physics-based description of ageing processes [11], and physical description of thermal behavior of the cell [9]. We report here the governing equations for the diffusion processes in the two electrodes and the equation describing the

cell voltage. Let the subscript $i = p, n$ denote the electrode (p and n respectively refers to the positive and negative), c_i ion concentration within the single particle as a function of time t and radial coordinate r , D_i diffusion coefficient of the electrode, S_i electrode total active surface and R_i radius of the particles composing the active material. Finally, I_{app} is the current applied to the cell, and F Faraday constant. The diffusion within the electrode active material is modeled through two radial partial differential equations:

$$\frac{\partial c(r, t)}{\partial t} = \frac{D_i}{r^2} \frac{\partial}{\partial r} \left(r^2 \frac{\partial c(r, t)}{\partial r} \right) \quad (1)$$

with boundary conditions:

$$D_i \frac{\partial c}{\partial r} \Big|_{r=0} = 0, \quad D_i \frac{\partial c}{\partial r} \Big|_{r=R} = \frac{I_{app}}{F S_i}, \quad (2)$$

These equations define the concentration of Lithium ions within the two electrodes. The external voltage of the cell V_{cell} is then computed as a sum of several terms, as in (3). U_p and U_n are the open circuit potential (OCP) of the cathode and anode, respectively, and are functions of the ion concentrations. η_p and η_n are the overpotentials due to the charge transfer in the cathode and anode respectively and are given by algebraic functions of the applied current and of the ion concentrations. $I_{app} R_{cell}$ describes the ohmic losses in the electrolyte. The equations and their terms are described in detail in [9].

$$\begin{aligned} V_{cell} = & + U_p(c_{p,surf}) + \eta_p(I_{app}, c_{p,surf}) \\ & - U_n(c_{n,surf}) + \eta_n(I_{app}, c_{n,surf}) \\ & + I_{app} R_{cell} \end{aligned} \quad (3)$$

III. INTEGRATION OF THE SPM IN A MPC FOR THE ENERGY MANAGEMENT OF A BESS

We consider the problem of controlling a BESS with the objective of achieving an assigned energy throughput in a given time horizon. This is a common application in the context of BESS energy management, see for example [6], [12], [13]. Remarkably, by taking advantage of the fact that the objective is achieving an integral quantity, one could think of implementing a MPC algorithm to determine an optimal current trajectory that, within the available time horizon, satisfy the control objective while obeying to BESS limits. BESS operational limits are enforced by the SPM model described above, which is linearized as described in the following.

A. Reformulation of the SPM

For the integration in such context, the SPM is linearized and expressed as the the following state-space form:

$$\begin{aligned} x_{k+1} &= A x_k + B u_k \\ y_{k+1} &= C x_{k+1} + D u_k \end{aligned} \quad (4)$$

The state vector x_k is composed by the ion concentration profiles in the two electrodes, provided by the diffusion equations and by the electrode overpotential values η_n and

η_p . The input u_k is the current applied to the cell I_{app} , and the output y_k is the cell voltage. With regard to the SPM equations, diffusion PDEs in (1) are discretized through a forward Euler scheme. The resulting linear equations provides the ion concentrations in the electrodes at each time step and at equally spaced positions along the particle radial coordinate r . The equations for the electrode overpotentials η_n and η_p and for the external voltage in (3) are nonlinear algebraic functions of the applied current I_{app} and ion concentration values in the two electrodes at $r = R$. They are therefore linearized with a first-order Taylor approximation around the working point at each time step, i.e. at each time step the system matrices of (4) are recomputed on the basis of the last known values of the SPM states.

B. MPC Formulation

As mentioned in the preamble of this section, we consider a MPC to achieve an assigned energy throughput in a available time horizon. Let $(1, 2, \dots, \bar{k})$ be the time horizon (of length \bar{k} and discretized at T_s seconds) for which the control trajectory is to determine, $k = 1, \dots, \bar{k}$ rolling index denoting the current time interval, e_k the reference BESS energy throughput to achieve by the end of the time window, and $\mathbf{i}_{k|k} = (i_{k|k}, i_{k+1|k}, \dots, i_{\bar{k}|k})$ sequence of BESS current values considered at time k . Assumed being at time k , the optimization problem underlying the adopted MPC is given by seeking the current profile to minimize the distance between the battery energy throughput and its reference tracking error at the end of the control, while subject to constraints on the current magnitude and concentration. Formally, it is:

$$\mathbf{i}_{k|k}^o = \arg \min_{\mathbf{i}_{k|k} \in \mathbb{R}^{(\bar{k}-k)}} \left\{ \left(\sum_{j=k}^{\bar{k}} (P_{j|k}) - e_k \right)^2 \right\} \quad (5)$$

subject to

$$P_{j|k} = v_{j|k} \cdot i_{j|k}, \quad j = k, \dots, \bar{k} \quad (6)$$

$$\mathbf{v}_{k|k} = f(x_{k|k}, \mathbf{i}_{k|k}) \quad (7)$$

$$\mathbf{x}_{k|k} = g(x_{k|k}, \mathbf{i}_{k|k}) \quad (8)$$

$$c_{i,j|k} \subset x_{j|k} \quad j = k, \dots, \bar{k} \quad (9)$$

$$\eta_{i,j|k} \subset x_{j|k} \quad j = k, \dots, \bar{k} \quad (10)$$

$$c_{i,min} \leq c_{i,j|k} \leq c_{i,max} \quad j = k, \dots, \bar{k} \quad (11)$$

$$\eta_{i,min} \leq \eta_{i,j|k} \leq \eta_{i,max} \quad j = k, \dots, \bar{k} \quad (12)$$

where (6) states that the BESS power output $P_{j|k}$ is the product between voltage $v_{j|k}$ and current $i_{j|k}$, (7) corresponds to the BESS voltage linearized model and, together with (8) composes the linearized state-space SPM. Equations (9) and (10) simply denote that the ion concentrations and the overpotentials in the electrodes are extracted as subsets of the state vector. Finally, (11) and (12) constrains concentrations and the overpotentials in the allowed ranges, denoted by $(c_{i,min}, c_{i,max})$ and $(\eta_{i,min}, \eta_{i,max})$. The former is imposed to avoid oversaturation or depletion of Lithium in the active

material of the two electrodes, while the latter bounds the overpotentials in each electrode, since excessive values would lead to the occurrence of deleterious conditions.

At each step k , the optimization problem is solved on a shrinking horizon k to \bar{k} and only the first portion of the optimal control $\mathbf{i}_{k|k}^o$ law is actuated. The computation of the evolution of the state vector requires the knowledge on the full state, which is reconstructed by applying a Kalman filter by using the measurements of the BESS DC voltage.

IV. SIMULATION SETUP AND RESULTS

A. Simulation setup

We consider a setup where a BESS is required to compensate for the mismatch between a dispatch plan at 5 minute resolution and the realization of a group of stochastic prosumers. The tracking problem is performed with the MPC described in Section III, which is augmented with the electrochemical predictive constraints (11)-(12). The mismatch enters in the problem as the input variable e_k , $\bar{k} = 5$ min and $T_s = 10$ s. The considered BESS is a 560 kWh unit, modelled as composed of $N_p = 18$ parallel branches, each with $N_s = 300$ Li-ion cells in series. These are 30 Ah MCMB-LiCoO₂ cells, with operating voltage between 3.6 and 4.1 V. At this stage, we assume that all the cells are balanced and have same physical properties¹. For such setup, and for each scenario detailed in the following sections, we perform two simulations. The first is obtained by solving a running an MPC in which the constrained quantities are the cell output voltage and current. In the second, we constrain the ion concentrations and electrode overpotentials instead. In both cases the prediction of the constrained quantities is based on the SPM described in section II². In both cases, at each simulation time step, the following actions are performed: *i*) a SPM-based Kalman filter reconstructs the state starting from measured current and voltage values, *ii*) based on the full knowledge of the state, the MPC optimization problem is solved and the first portion of the computed control action is chosen for being actuated, *iii*) BESS behavior as a function of the actuated current set-point is simulated through a detailed electrochemical model (described in [4]) at 500 ms resolution. The cell parameters of both the SPM used in the control and the detailed cell model used to simulated the battery behavior are from the literature [4].

In order to achieve a fair comparison between concentration and voltage limits, these have been selected in the following way. Concentration limits $c_{a,min}$, $c_{a,max}$, $c_{c,min}$ and $c_{c,max}$ are given as parameters of the model, i.e. they are the maximum and minimum Lithium stoichiometry achievable in

¹This allows to define $V_{BESS} = V_{cell} * N_s$ and $i_{BESS} = i_{cell} * N_p$.

²For the conventional MPC, simpler models, such as equivalent circuits, can fulfill the task of predicting the constrained quantities (i.e. currents and voltages). However, in the present work, both the conventional approach and the physics-based control rely on the same model (i.e. the SPM). In this way a fair comparison of their performances is possible.

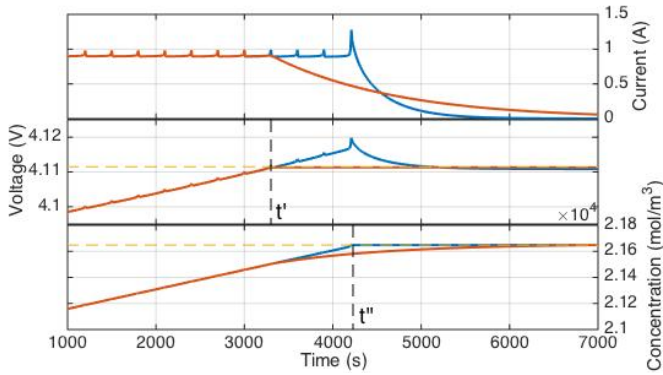


Figure 3. Battery charge with a fixed power set-point. **Top:** cell current, **middle:** cell voltage, **bottom:** anode surface ion concentration. Red lines refer to an MPC based on I-V limits, blue lines refer to a physics-based MPC. Yellow dashed lines in the middle and bottom plots represent the thresholds for the voltage and anode concentration respectively.

the electrodes. Voltage limits V_{max} and V_{min} are chosen to be equal to the open circuit voltages in correspondence of the extreme concentration conditions. Formally, $V_{min} = V_{oc}(c_{a,min}, c_{c,max})$ and $V_{max} = V_{oc}(c_{a,max}, c_{c,min})$. This is because the relation between voltage and concentrations is not time-invariant. The selected voltage limits are chosen so that concentration limits (where the concentration is the quantity that we *really* want to constrain) are not violated in any condition, i.e. for any shape of input current profile. For a fast charge, for example, the instantaneous voltage will be higher than the open circuit voltage of the cell corresponding to a given set of concentrations. Thus, a voltage limit will be conservative compared to the concentration limits. For a very slow charge, the instantaneous voltage will be almost equal to the open circuit voltage and the voltage limit will represent well the cell concentration limitations.

Figure 3 is useful to understand this link: it shows the current, voltage and anode surface ion concentration in a trivial scenario in which the controller requires to the cell to be charged as much as possible at a constant current rate. Red lines refer to the case in which in the controller voltage and current are constrained. A constant-current charge is interrupted at t' and a constant-voltage charge takes place. The blue lines refer to the case in which concentrations and overpotentials are constrained. The constant-current charge can therefore continue even for voltages that are higher than the threshold of the previous case, as concentration limits are not violated. When these are reached at t'' , a constant-concentration charge takes place. It can be seen, the constant voltage and constant concentration charges lead to the same cell state for long charging times. The current decreases and the charge continues closer and closer to an equilibrium condition, at which the two limits coincide. Nevertheless, it is also evident that in the case where the constrained quantities are the concentrations rather than the voltage, the constant-current charge can continue longer. This is an actual improvement in the cell performances, since the range in which the cell can provide the desired

current is enlarged.

B. Results

1) *Analysis at different power rates:* We first run a set of simulations such the one in Fig. 3 for a set of power values, in order to assess the performances of the new control paradigm at various power rates. For any power setpoint we run both a simulation using an MPC based on I-V limits and one on the electrochemical constraints defined above. For each couple of simulations the metrics chosen to perform the comparison are the following: *i)* ΔT : the delay, in minutes, between the constraint activation in the case of PB control and of MPC based on I-V limits; *ii)* ΔE : the increase in the energy delivered at the desired power (i.e. in unconstrained operation), with regard to the cell nominal capacity; *iii)* oV : the cell overvoltage in mV reached in the case of PB control, over traditional control; *iv)* C_{ratio} : anode surface ion concentration reached at constraint activation with traditional I-V limits (relative to the case of PB control). Table I shows the results of such simulations for a set of charge values.

Table I
COMPARISON METRICS FOR BESS CHARGE

Power (p.u.)	ΔT (min)	ΔE (%)	oV (mV)	C_{ratio}
0.01	10.2	0.12	1.07	1
0.02	14.8	0.41	2.67	1
0.04	15.5	1.03	5.91	0.99
0.06	15	1.3	8.67	0.99
0.08	15.5	2	12.29	0.99
0.1	15.3	2.43	14.84	0.98
0.15	14.8	3.59	18.44	0.98
0.2	14.2	3.63	22.68	0.97
0.3	15	7.24	35.37	0.95
0.4	17.7	11.03	47.54	0.92
1	10	20.64	81.54	0.9

2) *Comparison for a realistic scenario:* Finally, we simulated a realistic daily scenario of BESS operation, considering the application described in [6]. The MPC control framework with I-V limits has been used to control a grid-connected BESS in order to dispatch the operation of a distribution feeder according to a trajectory with 5 minutes resolution, established the day before the operation. The data used for this simulation are from the operation of the 15th of January 2016. In such day, the tracking of the objective dispatch plan failed due to the BESS hitting its upper voltage limits.

We show in this section the results obtained simulating the operation of the BESS, controlled via an MPC in which classical I-V limits are implemented and one based on a PB control. Notably, Fig. 4 shows the tracking performances of the two MPCs. Both achieve perfect tracking for most of the analysed day. Nevertheless, due to considerable charging demand in the first part of the day, around midday both control approaches fail in their objective. Table II shows the performances relative to the two constrained control implementations. We observe that, while the BESS fails to track the dispatch plan along

Table II
COMPARISON OF THE TWO CONTROL APPROACHES FOR A DAY OF OPERATION

I-V limits		
Tracking fails during:	21	min
Cumulated tracking error:	17.88	kWh
Physics-based control		
Tracking fails during:	18	min
Cumulated tracking error:	11.59	kWh

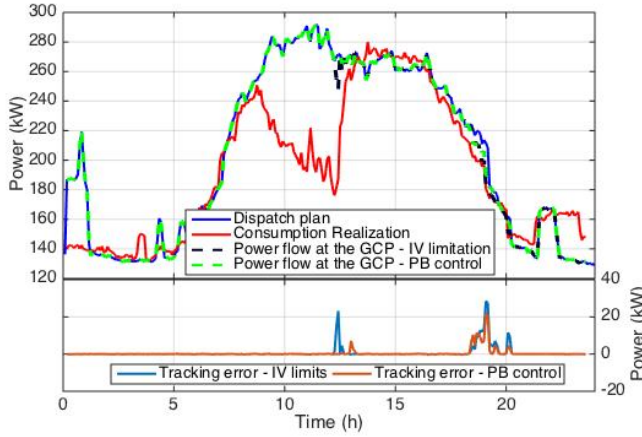


Figure 4. **Top:** 5-minute resolution profiles of reference power profile, power realization and corrected power profile (both conventional and physics-based MPC). **Bottom:** Tracking error.

the whole day in both cases, in the case of PB control the time interval during which the tracking objective is not respected decreases. Most importantly, the cumulated tracking error along the day decreases considerably (of about the 35%), i.e. even when the tracking fails, the tracking error achieved by the physics based control is reduced. Fig. 5 shows in the first two panels the simulated current and voltage profiles during 24 hours of operation (for the case of PB-MPC). In the third panel of Fig. 5 it is shown the voltage prediction error. It can be seen that the SPM achieves a good performance in voltage prediction, with a relative maximum error well below 0.5%. Finally, Fig. 6 shows, in the top panel, the ion concentration profile relative on the surface of the anode particle together with its respective constraints, and, in the bottom panel, the current density of the side reaction leading to SEI formation. The latter has been calculated from the quantities made available by the SPM and by implementing the model in [14] and is of definite importance because it opens to the inclusion in the MPC of anti-ageing policies.

C. Discussion

Table II shows how, for a real-world BESS application and a realistic scenario, physics based control can achieve better

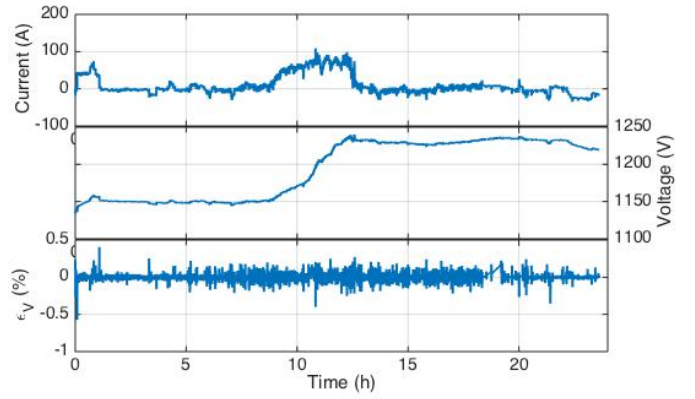


Figure 5. **Top:** BESS current profile simulated through the detailed electrochemical model. **Middle:** BESS simulated voltage profile. **Bottom:** One-step-ahead prediction error of the voltage predicted through the SPM.

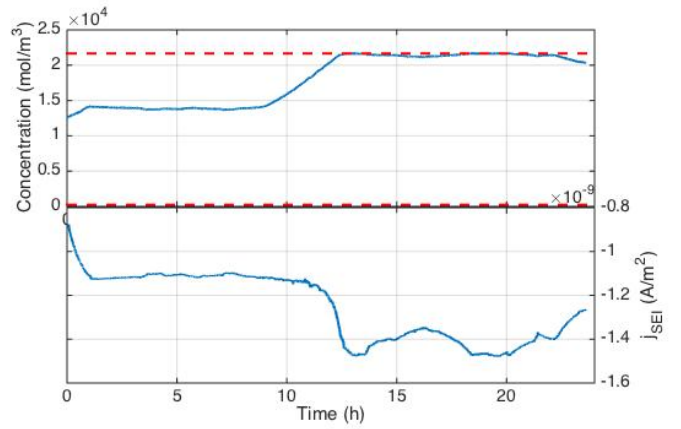


Figure 6. **Top:** Profile of the ion concentration at the anode particle surface (blue line) and its boundaries (red dashed lines). **Bottom:** Profile of the current density of the parasitic reaction leading to SEI formation.

performances compared to standard approaches. The advantage of the proposed approach is particularly conspicuous for higher power rates (as shown in Table I) which may provide a considerable advantage in high-power BESS applications.

Knowledge of ion concentrations and potentials within the cells, besides allowing for their direct limitation, allows to limit explicitly the magnitude of side reactions that induce capacity fade and increase in the equivalent series resistance. The magnitude of these side reactions is in fact dependent on the values of the internal states provided by the PB model. Therefore leaning on a PB model, one can integrate explicit models of these side reaction as well, rather than relying on heuristic approaches to limit degradation.

As an example, we discuss hereafter SEI formation, which is one of the more common of such degradation mechanisms. SEI formation consists in the irreversible consumption of cyclable Lithium via a side reaction between Lithium and solvent species present in the electrolyte that takes place at

the surface of the anode-material particles. This causes a fade in the cell capacity and an increase in the cell resistance (i.e. a degradation in the cell capability to provide high power values). This mechanism is common to most Li-ion cell chemistries and has been widely studied [15], [16]. In [14] a reduced order model for SEI formation is formulated. The current density of the side reaction j_{SEI} is provided by a non-linear function of the anode intercalation current and of the negative electrode equilibrium potential. Since in the SPM the intercalation current is proportional to the cell current and the negative equilibrium potential is a function of anode surface concentration, it is possible, via the SPM and the proposed control framework, to explicitly limit the operating range so that j_{SEI} remains below a desired threshold.

V. CONCLUSION

We propose a model predictive control for a battery energy storage system (BESS) where BESS operation constraints are enforced through electrochemical constraints implemented through a predictor based on the single particle model. With respect to conventional control policies based on feedback control loops and MPC based on equivalent circuit models, the proposed solution achieves an augmented awareness of the control process thanks to a detailed representation of electrochemical dynamics. Conventional current and voltage constraints are replaced in favor of overpotential and concentration constraints, which allows for a more efficient exploitation of the BESS true capacity while accounting for aging.

We compare the performance of a control scheme based on traditional current/voltage limitations and one exploiting SPM electrochemical predictions. We show how, for an energy management application the proposed control scheme achieves better performances when compared to one based on classical current-voltage limitations. Notably, tracking error decreases, in the first case of about the 35% with respect to the latter. Via the simulation of a set of constant current charges, we show as well how PB control achieves better performances, allowing for a charge/discharge at the desired rate for a longer time, while respecting the battery real limitations. This corresponds to an extension of the operating range of the battery, which is particularly remarkable for high current values. The latter result indicate that the proposed approach may be particularly convenient for BESS high-power applications.

ACKNOWLEDGEMENTS

This research received funding from the Swiss Competence Center for Energy Research (FURIES), Romande Energie and Swiss Vaud Canton within the initiative “100 millions pour les énergies renouvelables et l’efficacité énergétique”.

REFERENCES

[1] N. A. Chaturvedi, R. Klein, J. Christensen, J. Ahmed, and A. Kojic, “Algorithms for advanced battery-management systems,” *IEEE Control Systems*, vol. 30, no. 3, pp. 49–68, 2010.

[2] K. A. Smith, C. D. Rahn, and C.-Y. Wang, “Model-based electrochemical estimation and constraint management for pulse operation of lithium ion batteries,” *IEEE Transactions on Control Systems Technology*, vol. 18, no. 3, pp. 654–663, 2010.

[3] D. J. Docimo, M. Ghanaatpishe, M. J. Rothenberger, C. D. Rahn, and H. K. Fathy, “The lithium-ion battery modeling challenge: a dynamic systems and control perspective,” *Mechanical Engineering*, vol. 136, no. 6, p. S7, 2014.

[4] S. J. Moura, “Estimation and control of battery electrochemistry models: A tutorial,” in *2015 54th IEEE Conference on Decision and Control (CDC)*. IEEE, 2015, pp. 3906–3912.

[5] H. Perez, N. Shahmohammadhamedani, and S. Moura, “Enhanced performance of li-ion batteries via modified reference governors and electrochemical models,” 2015.

[6] F. Sossan, E. Namor, R. Cherkaoui, and M. Paolone, “Achieving the dispatchability of distribution feeders through prosumers data driven forecasting and model predictive control of electrochemical storage,” *IEEE Transactions on Sustainable Energy*, vol. 7, pp. 1762–1777, 2016.

[7] B. Hredzak, V. G. Agelidis, and G. Demetriades, “Application of explicit model predictive control to a hybrid battery-ultracapacitor power source,” *Journal of Power Sources*, vol. 277, pp. 84–94, 2015.

[8] S. Teleke, M. E. Baran, S. Bhattacharya, and A. Q. Huang, “Optimal control of battery energy storage for wind farm dispatching,” *IEEE Transactions on Energy Conversion*, vol. 25, no. 3, pp. 787–794, 2010.

[9] M. Guo, G. Sikha, and R. E. White, “Single-particle model for a lithium-ion cell: Thermal behavior,” *Journal of The Electrochemical Society*, vol. 158, no. 2, pp. A122–A132, 2011.

[10] S. J. Moura, F. B. Argomedo, R. Klein, A. Mirtabatabaei, and M. Krstic, “Battery state estimation for a single particle model with electrolyte dynamics,” *IEEE Transactions on Control Systems Technology*, 2016.

[11] G. Ning, R. E. White, and B. N. Popov, “A generalized cycle life model of rechargeable li-ion batteries,” *Electrochimica acta*, vol. 51, no. 10, pp. 2012–2022, 2006.

[12] M. Marinelli, F. Sossan, G. T. Costanzo, and H. W. Bindner, “Testing of a predictive control strategy for balancing renewable sources in a microgrid,” *IEEE Transactions on Sustainable Energy*, vol. 5, no. 4, pp. 1426–1433, Oct 2014.

[13] M. Abu Abdullah, K. Muttaqi, D. Sutanto, and A. Agalgaonkar, “An effective power dispatch control strategy to improve generation schedulability and supply reliability of a wind farm using a battery energy storage system,” *Sustainable Energy, IEEE Transactions on*, vol. 6, 2015.

[14] A. V. Randall, R. D. Perkins, X. Zhang, and G. L. Plett, “Controls oriented reduced order modeling of solid-electrolyte interphase layer growth,” *Journal of Power Sources*, vol. 209, pp. 282–288, 2012.

[15] D. Aurbach, B. Markovsky, M. Levi, E. Levi, A. Schechter, M. Moshkovich, and Y. Cohen, “New insights into the interactions between electrode materials and electrolyte solutions for advanced nonaqueous batteries,” *Journal of power sources*, vol. 81, pp. 95–111, 1999.

[16] P. Ramadass, B. Haran, P. M. Gomadam, R. White, and B. N. Popov, “Development of first principles capacity fade model for li-ion cells,” *Journal of the Electrochemical Society*, vol. 151, no. 2, pp. A196–A203, 2004.